View metadata, citation and similar papers at core.ac.uk

brought to you by CORE

東北大学機関リポジトリ
TOUR
Tohoku University Repository

Pair-Ion Plasma Generation using Fullerenes

著者	畠山　力三
journal or publication title	Physical review letters
volume	91
number	20
page range	205005-1-205005-4
year	2003
URL	http://hdl.handle.net/10097/35107

doi: 10.1103/PhysRevLett.91.205005

VOLUME 91, NUMBER 20 PHYSICAL REVIEW LETTERS week ending 14 NOVEMBER 2003

Pair-Ion Plasma Generation using Fullerenes

Wataru Oohara and Rikizo Hatakeyama

Department of Electronic Engineering, Tohoku University, Sendai 980-8579, Japan

(Received 17 April 2003; published 14 November 2003)

We have developed a novel method for generating pure pair plasma which consists of positive- and negative-charged particles with an equal mass. The pair-ion plasma without electrons is generated using fullerene as an ion source through the processes of hollow-electron-beam impact ionization, electron attachment, preferential radial diffusion of ions, and resultant electron separation in an axial magnetic field. Basic characteristics of this plasma are discussed in terms of the differences from ordinary electron-ion plasmas, such as a phenomenon in the absence of sheath and potential structure formation.

DOI: 10.1103/PhysRevLett.91.205005 PACS numbers: 52.27.Ep, 52.50.Dg, 81.05.Tp

Ordinary plasmas consist of electrons and positive ions, and the mass difference between negative- and positive-charged particles essentially causes temporal and spatial varieties of collective plasma phenomena. If several species of ions exist in plasmas, phenomena in the plasma are diversified and become complicated. It has widely been recognized that plasmas containing dust or fine particles are a subject of intensive study in various fields of physics and engineering such as space astrophysics [1,2], plasma physics [3], plasma-aided manufacturing [4,5], and fusion technology [6,7]. The dust or fine particles are negatively charged in low-temperature plasmas. The plasmas including massive negative ions with mass much heavier than that of positive ions are confirmed to exist in many natural and technological settings. The negative-ion plasmas have been generated in laboratories by various methods in order to investigate wave and instability phenomena [8–10]. Also the electron-free plasma consisting of negative and positive ions (I^- and Tl^+) with an unequal mass was produced by photodissociation of molecular TlI and confined in a Paul rf quadrupole electric field [11].

On the other hand, contrary to the trend of the research mentioned above, pair plasmas consisting of only positive- and negative-charged particles with an equal mass have been investigated experimentally [12–14] and theoretically [15]. In pair plasmas, such as an electron-positron plasma, attention has been focused largely on the relativistic and/or nonrelativistic regime, since such plasmas are thought to be generated naturally under certain astrophysical conditions. Pair plasmas represent a new state of matter with unique thermodynamic property drastically different from ordinary plasmas. A number of experimental approaches have been proposed for studying electron-positron plasmas in the laboratory. The electron-positron plasma is experimentally generated by injecting a low-energy electron beam into the positron plasma which is obtained by scattering from a buffer gas into a Penning trap and stored at densities of more than 10^7 cm^{-3}. A comprehensive analysis of the elementary properties of pair plasmas, linear-, and nonlinear-collective plasma modes was theoretically developed [16] and the experimental identification is desired to be performed. However, pair annihilation can take place in two-body collisions and via positronium atom formation. It is necessary for long-time-scale plasma physics experiments to meet the condition that the annihilation time scale is many orders of magnitude larger than the plasma period. In order to maintain a steady state plasma over such long times the pairs are needed to be created prolifically to balance the annihilation rate because they annihilate on short time scales (10^{-14}–10^{-11} cm^3 s^{-1}). Thus, it is not easy to generate and maintain the electron-positron plasma, and therefore our attention is concentrated on the easy and steady state generation of a pair-ion plasma consisting of positive and negative ions with an equal mass.

According to our previous work on the generation of an alkali-fullerene plasma (K^+, e^-, C_{60}^-) by introducing a fullerene into a potassium plasma [17,18], fullerenes are adopted as a candidate for the ion source in order to realize the pair-ion plasma, based on the fact that the interaction of electrons with the fullerenes leads to the production of both negative [19,20] and positive [21,22] ions. In this Letter, we describe an experiment which has achieved the steady state generation of the pair-ion plasma using the fullerenes.

A conventional dc discharge plasma source with a vacuum chamber of 15.7 cm in diameter and 260 cm in length is modified to function as a pair-ion plasma source with ion species of fullerenes, as shown schematically in Fig. 1. A uniform magnetic field of $B = 0.3$ T is applied by solenoid coils and the background gas pressure is 2×10^{-4} Pa. A copper cylinder (10 cm in diameter and 30 cm in length) with a copper annulus (inner diameter 3 cm, outer diameter 10 cm, and 0.1 cm in thickness) is fixed inside a cylindrical ceramic furnace and heated to 500 °C. A ceramic cathode of a 10-cm-diam LaB_6 disk at $z = 0$ cm is radiatively heated from behind to approximately 1500 °C by a tungsten wire heater. A grounded grid is set in front of the cathode and the distance between the cathode and the grid can be minutely

© 2003 The American Physical Society

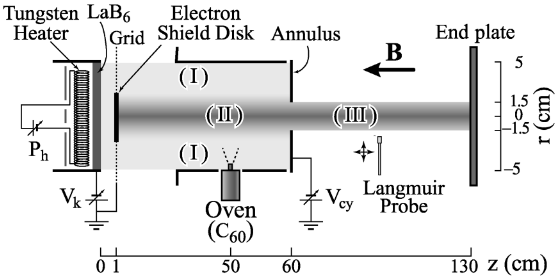

FIG. 1. Schematic drawing of the experimental setup. An electron beam for ionization takes the form of a hollow tube. Pure pair-ion plasma using a fullerene (C_{60}^+, C_{60}^-) is generated by electron-impact ionization, electron attachment, and preferential diffusion of ions.

adjusted in the range less than 1 cm. The cathode is biased at a voltage V_k with respect to the ground. Low-energy electrons ($\sim$0.1 eV), thermionically emitted from the cathode, are accelerated by an electric field between the cathode and the grid, forming an electron beam. The electron-beam energy can be controlled in the range of 0–150 eV with an accuracy of 0.1 eV by changing V_k. A stainless-steel disk (6 cm in diameter) is installed on the grid; therefore the shape of the electron beam becomes a hollow tube. The hollow electron beam flows along magnetic field lines and is terminated at the annulus. The copper cylinder is grounded and the annulus can be independently biased at a voltage V_{cy}. The chamber wall is grounded and the end plate is kept at a floating potential. For analytic convenience, the whole space of this plasma source is divided into three regions. The electron-beam region is called region (I) as a fullerene-ion production region. The cylinder and the ceramic furnace have a hole (3 cm in diameter) on the sidewall and an oven for fullerene sublimation is set there. A fullerene sample, which is commercially available C_{60} powder of 99.5% purity, is heated in the oven. Typical oven temperatures under operating conditions range between 400 and 600 °C. The fullerene vapor produced as a result of sublimation is effused through a 0.3-cm-diam hole under molecular flow conditions, filling region (I).

The attachment cross-section function for the production of C_{60}^- has been determined as a function of electron energy. Free-electron attachment occurs over a very broad-energy range, extending to 12 eV. The attachment cross-section curve for the reaction $C_{60} + e^- \rightarrow C_{60}^-$, $\sigma(C_{60}^-)$, exhibits a distinct low-energy threshold ($\sim$0.15 eV). The cross-section value is $\sigma(C_{60}^-) = 100 \times 10^{-24}$ cm^2 at 0.5 eV. The ionization cross-section curve for the reaction $C_{60} + e^- \rightarrow C_{60}^+ + 2e^-$, $\sigma(C_{60}^+)$, does not show any precipitous structure. The cross-section value is $\sigma(C_{60}^+) = 25 \times 10^{-24}$ cm^2 at 100 eV. The electron-impact ionization of C_{60} gives rise to a variety of different ions, including stable parent ions, stable fragment ions, and metastable parent or fragment ions. The electron energy dependence of the production of singly and multiply charged parent and fragment ions has been investigated. When C_{60}^+ are produced by the electron-impact ionization, low-energy electrons are simultaneously produced in connection with the process and they contribute to produce negative ions. Negative ions produced by the electron attachment are singly charged due to the size, and the process is simple compared with the electron-impact ionization. It is a key in producing concurrently C_{60}^+ and C_{60}^- that C_{60} has a feature of the electron attachment over the broad-energy range. Charged-particle gyroradii are in proportion to $\sqrt{\text{mass}}/\text{charge}$ ratio. The gyroradii of C_{60}^+ and C_{60}^- are larger than those of e^-, C_{60}^{2+}, C_{60}^{3+}, C_{58}^+, C_{56}^+, etc., if their kinetic energies perpendicular to the B-field lines are the same. The gyroradius ratio $\rho_{C_{60}^+}/\rho_{e^-}$ is especially high ($\simeq$1100). A preferential diffusion of C_{60}^+ and C_{60}^- can take place in the radial (r) direction across the B-field lines due to their large gyroradii, i.e., a magnetic-filtering effect. Only C_{60}^+ and C_{60}^- are expected to exist in region (II) behind the electron-shield disk because the production rates of the other ions are much lower and their gyroradii are smaller. C_{60}^+ and C_{60}^- flow along the B-field lines and pass through the annular hole. Thus, the electron-free pair-ion plasma (C_{60}^+, C_{60}^-) generation is attained in region (III) downstream from the annulus. Plasma parameters in region (III) are measured by Langmuir probes, collectors of which are prevented from contamination of C_{60}.

The generation property of the pair-ion plasma depending on the electron-beam energy is measured at $r = 0$ cm and $z = 65$ cm for $V_{cy} = 0$ V, as shown in Fig. 2(a). I_+ and I_- are the Langmuir-probe saturation currents of C_{60}^+ and C_{60}^-, which are collected for -50 and 50 V of the probe voltages V_p applied with respect to the ground, respectively. The saturation currents are considered to be in proportion to the plasma density. ϕ_f is the floating potential of the probe. A typical current (I_p)-voltage (V_p) (solid line) and differentiated (dI_p/dV_p, dotted line) characteristics of the probe are displayed in Fig. 2(b) for the electron-beam energy of 100 eV. When the electron-beam energy increases and exceeds a threshold ($>$30 eV) in Fig. 2(a), the saturation currents begin to increase, i.e., the pair-ion plasma begins to be generated. The plasma density gradually increases, almost saturates around 70 eV, and attains to 2×10^7 cm^{-3} at 100 eV. The temperature of C_{60}^+ (T_+) increases in proportion to the electron-beam

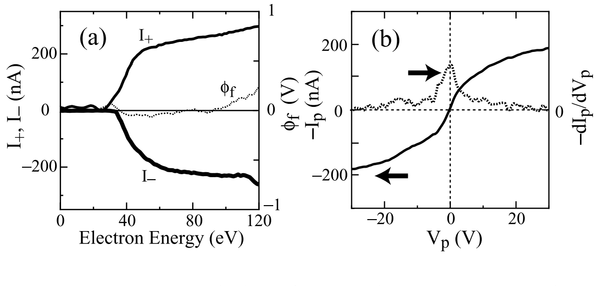

FIG. 2. (a) Characteristic of C_{60} discharge depending on electron-beam energy. (b) Typical current-voltage characteristic of Langmuir probe is displayed (electron energy: 100 eV).

energy up to 1.5 eV at 100 eV. The floating potential is measured to be slightly positive ($>$90 eV) because the temperature of C_{60}^+ becomes slightly higher than that of C_{60}^- (T_-). As seen in Fig. 2(b), the I_p-V_p characteristic is symmetrical with respect to the ground voltage and the zero current. V_p yielding a peak of the differential profile indicates the plasma potential and almost coincides with the floating potential. Since the plasma potential is almost 0 V which is equal to the potential of the grid and annulus, it can be said that there is no axial potential structure in the plasma and even a sheath is not formed in front of the boundary layer such as a plasma end plate interface. And the positive and negative saturation currents of the characteristic are shown to be approximately equal. If electrons measurably exist in the plasma, the negative current would be bigger than the positive current, and the sheath would be formed. Thus the existence of electrons in the pair-ion plasma can be negligible.

In order to know what kind of ions exist in the pair-ion plasma, ion species are analyzed by using an omegatron analyzer [23] in a strong magnetic field which is applied by superconducting coils. Since two collectors are set in the analyzer, the surfaces of which are faced in the opposite direction perpendicular to the B-field lines, the collector currents of positive and negative ions can easily be distinguished because the gyration directions of both the ions are absolutely opposite. The collector current of the analyzer is plotted (not shown) as a function of frequency of radio-frequency electric field applied for cyclotron acceleration. This frequency spectrum has a clear peak. A dependence of the frequency giving the peak on the magnetic field ($B = 1$–1.6 T) shows a good agreement with predicted values of the cyclotron frequency for C_{60}^+ or C_{60}^- ($\omega_c/2\pi = 21.3$ kHz for $B = 1$ T). It is to be noted that no other peaks except the C_{60} peaks are observed in the spectra. Thus, we can conclude that positive and negative ions in the pair-ion plasma are C_{60}^+ and C_{60}^-, not C_{60}^{2+} and C_{60}^{2-}, etc.

The spatial distribution of the probe-saturation current of positive ions (I_+) is measured in region (III) and described on a two-dimensional (r-z) plane as shown in Fig. 3, indicating the spatial variation of the plasma density. Since the distribution of I_- is almost the same as that of I_+, I_- is not shown here. The ions rapidly diffuse and the plasma diameter becomes larger than the annular-hole diameter of 3 cm. The radial profile of the plasma density is Gaussian and the density at $r = 0$ cm on the axis decreases gradually toward the region downstream from the annular hole because of the radially outward diffusion across the B-field lines. The density gradient on the axis is -4.5×10^5 cm^{-4} and the density becomes half per $\Delta z = 22$ cm. Typical plasma parameters in the pair-ion plasma [$B = 0.3$ T, $T \equiv T_+ = T_- = 1.5$ eV (isotropy), $n \equiv n_+ = n_- = 2 \times 10^7$ cm^{-3}] are obtained as follows: the pair-ion plasma frequency $\omega_{pp}/2\pi \equiv (\omega_{p+}^2 + \omega_{p-}^2)^{1/2}/2\pi = (2ne^2/\varepsilon_0 m)^{1/2}/2\pi = 49.6$ kHz, the cyclotron frequency $\omega_c/2\pi = 6.4$ kHz, the Debye length $\lambda_D \equiv (\varepsilon_0 k_B T/e^2 n)^{1/2} = 2 \times 10^{-3}$ m, and the gyroradius $\rho_L = v_\perp/\omega_c = 1.6 \times 10^{-2}$ m, where ε_0 is the permittivity of free space, $m \equiv m_+ = m_-$ is the mass of the ions, and k_B is the Boltzmann constant. The ions can easily diffuse because the applied magnetic field is weak for this pair-ion plasma ($\omega_c/\omega_{pp} = 0.13$), where the gyroradius is larger than the Debye length ($\rho_L/\lambda_D = 8$) and comparable to the plasma radius (inner diameter of the annulus is 3 cm), and the finite-Larmor-radius effect can no longer be neglected. The density nonuniformity is reduced to a considerable extent using a thick annulus ($0.1 \rightarrow 4$ cm), which in advance prevents the ions with the larger Larmor diameter from flowing downstream. Besides the application of a strong magnetic field in the range of tesla could be very effective to greatly reduce the density nonuniformity. The dominant reason for the density decrement is the diffusion, but the pair annihilation is considered to be also related. In an electron-positron plasma, the pair annihilation ($e^+ + e^- \rightarrow 2\gamma, 3\gamma, \ldots$) can take place. The pair-annihilation processes are of particular importance in astrophysics since the γ rays produced give a clear signature of the presence of positrons. The electron-positron plasma survives sufficiently long for many pair-plasma oscillations before it annihilates. In our pair-ion plasma, pair-ion annihilation probably takes place: $C_{60}^+ + C_{60}^- \rightarrow 2C_{60}$ (neutralization) and $C_{60}^+ + C_{60}^- \rightarrow C_{120}$ (dimerization). Especially in the case of C_{60} dimerization, the C_{60} dimer has acquired an interest from the standpoint of applications to nanoscale magnetic materials [24]. There have been many reports on the synthesis of C_{60} dimers using various kinds of methods: photoirradiation, high pressure and temperature, and mechanochemical reaction. For instance, the dumbbell-shaped dimer C_{120} can be synthesized by a solid-state mechanochemical reaction of C_{60} with potassium cyanide (KCN) [25]. The pair-ion plasma is expected to be used for the synthesis of the dimers directly from carbon allotropes. This method is quite different from current ones, accompanied by stepwise procedures in solid- or solution-phase reactions using catalysts or nonallotropic fullerene derivatives.

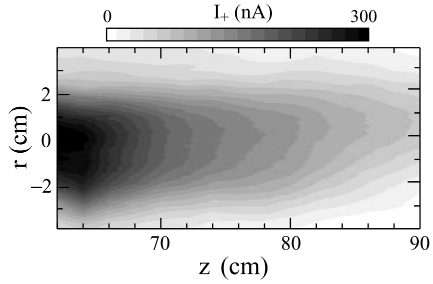

FIG. 3. Spatial (axial-radial) profile of pair-ion plasma density in the downstream region from the annulus.

In addition to the basic physical interest, the study of collective modes in the pair-ion plasma is of importance from the diagnostic point of view, since the observation of

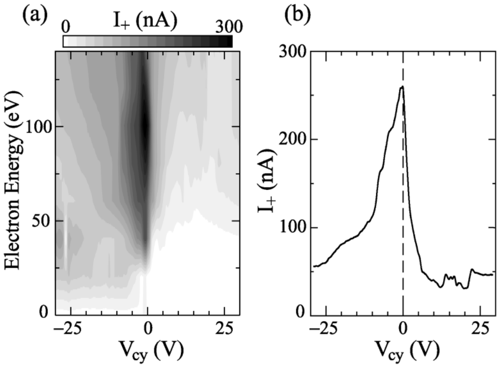

FIG. 4. (a) Pair-ion plasma density depending on electron-beam energy and annulus bias: voltage V_{cy}. (b) Positive-ion saturation current vs V_{cy} (electron energy: 100 eV).

propagation characteristics of the modes is used to determine precisely the plasma parameters. A comprehensive two-fluid model has been developed for collective-mode analyses in electron-positron plasmas, and longitudinal and transverse electrostatic and electromagnetic modes have been studied. The longitudinal collective modes are analogous to those in the ordinary electron-ion plasmas. On the other hand, the transverse collective modes in the presence of a magnetic field are quite different from those in the ordinary plasmas, for instance, the whistler mode does not exist. The I_+ distribution as functions of the annulus bias voltage V_{cy} and the electron-beam energy is shown in Fig. 4(a). At each electron-beam energy, I_+ is measured in the range between $V_{cy} = -30$ and 30 V. The darkness is in proportion to the intensity of I_+ (plasma density). Figure 4(b) gives a typical I_+ profile depending on V_{cy} at the beam energy of 100 eV. The results indicate that the plasma density decreases drastically for $|V_{cy}| >$ 0 V at any electron energy. This means that the density modulation (fluctuation) can be generated (excited) without using a grid immersed inside the plasma cross section, which disturbs the plasma condition, when V_{cy} is changed temporally. Thus, longitudinal-electrostatic modes will be easily measured in the pair-ion plasma since the density and the temperature are relatively low.

In summary, the generation of a pair-ion plasma, consisting of positive and negative ions with the equal mass without electrons, is performed using a hollow electron beam in a magnetic field, where electron-impact ionization and electron attachment play a key role. C_{60} with a stable cage is used as an ion source because it is easily charged positively (C_{60}^+) and negatively (C_{60}^-). A magnetic-filtering effect is used for the separation of electrons and the ions. In the pair-ion plasma, potential structures including sheaths are not formed and the ions rapidly diffuse across the B-field lines. This pair-ion plasma could be useful for the synthesis of C_{60} dimers and the investigation of linear and nonlinear behaviors of collective modes.

The authors would like to thank T. Hirata and T. Kaneko for their collaboration in the omegatron measurements. We are indebted to N. Tomioka, M. Kobayashi, and D. Date for their support. This work was supported by a Grant-in-Aid for Scientific Research from the Ministry of Education, Culture, Sports, Science, and Technology, Japan.

[1] C. K. Goertz, Rev. Geophys. **27**, 271 (1989).
[2] F. Verheest, Space Sci. Rev. **77**, 267 (1996).
[3] H. Thomas, G. E. Morfill, V. Demmel, J. Goree, B. Feuerbacher, and D. Mohlmann, Phys. Rev. Lett. **73**, 652 (1994).
[4] G. S. Selwyn, J. E. Heidenreich, and K. L. Haller, Appl. Phys. Lett. **57**, 1876 (1990).
[5] L. Boufendi, A. Bouchoule, P. K. Porteous, J. Ph. Blondeau, A. Plain, and C. Laure, J. Appl. Phys. **73**, 2160 (1993).
[6] A. Gondhalekar, P. C. Stangeby, and J. D. Elder, Nucl. Fusion **34**, 247 (1994).
[7] B. N. Kolbasov, A. B. Kukushkin, V. A. Rantsev-Kartinov, and P. V. Romanov, Phys. Lett. A **269**, 363 (2000).
[8] A. Y. Wong, D. L. Mamas, and D. Arnush, Phys. Fluids **18**, 1489 (1975).
[9] B. Song, N. D'Angelo, and R. L. Merlino, Phys. Fluids B **3**, 284 (1991).
[10] W. Oohara, S. Ishiguro, R. Hatakeyama, and N. Sato, J. Phys. Soc. Jpn. **71**, 373 (2002).
[11] J. P. Schermann and F. G. Major, Appl. Phys. **16**, 225 (1978).
[12] C. M. Surko, M. Leventhal, and A. Passner, Phys. Rev. Lett. **62**, 901 (1989).
[13] H. Boehmer, M. Adams, and N. Rynn, Phys. Plasmas **2**, 4369 (1995).
[14] E. P. Liang, S. C. Wilks, and M. Tabak, Phys. Rev. Lett. **81**, 4887 (1998).
[15] N. Iwamoto, Phys. Rev. E **47**, 604 (1993).
[16] G. P. Zank and R. G. Greaves, Phys. Rev. E **51**, 6079 (1995).
[17] N. Sato, T. Mieno, T. Hirata, Y. Yagi, R. Hatakeyama, and S. Iizuka, Phys. Plasmas **1**, 3480 (1994).
[18] W. Oohara, R. Hatakeyama, and S. Ishiguro, Plasma Phys. Controlled Fusion **44**, 1299 (2002).
[19] T. Jaffke, E. Illenberger, M. Lezius, S. Matejcik, D. Smith, and T. D. Märk, Chem. Phys. Lett. **226**, 213 (1994).
[20] J. Huang, H. S. Carman, Jr., and R. N. Compton, J. Phys. Chem. **99**, 1719 (1995).
[21] R. Völpel, G. Hofmann, M. Steidl, M. Stenke, M. Schlapp, R. Trassl, and E. Salzborn, Phys. Rev. Lett. **71**, 3439 (1993).
[22] S. Matt, B. Dünser, M. Lezius, H. Deutsch, K. Becker, A. Stamatovic, P. Scheier, and T. D. Märk, J. Chem. Phys. **105**, 1880 (1996).
[23] T. Hirata, R. Hatakeyama, Y. Yagi, T. Mieno, S. Iizuka, and N. Sato, J. Plasma Fusion Res. **71**, 615 (1995).
[24] E. E. B. Campbell, V. Schyja, R. Ehlich, and I. V. Hertel, Phys. Rev. Lett. **70**, 263 (1993).
[25] G.-W. Wang, K. Komatsu, Y. Murata, and M. Shiro, Nature (London) **387**, 583 (1997).